Article

Ultrafast Time-Resolved Study of Photophysical Processes Involved in the Photodeprotection of *p*-Hydroxyphenacyl Caged Phototrigger Compounds

Chensheng Ma, Wai Ming Kwok, Wing Sum Chan, Peng Zuo,
Jovi Tze Wai Kan, Patrick H. Toy, and David Lee Phillips

J. Am. Chem. Soc., **2005**, 127 (5), 1463-1472• DOI: 10.1021/ja0458524 • Publication Date (Web): 12 January 2005

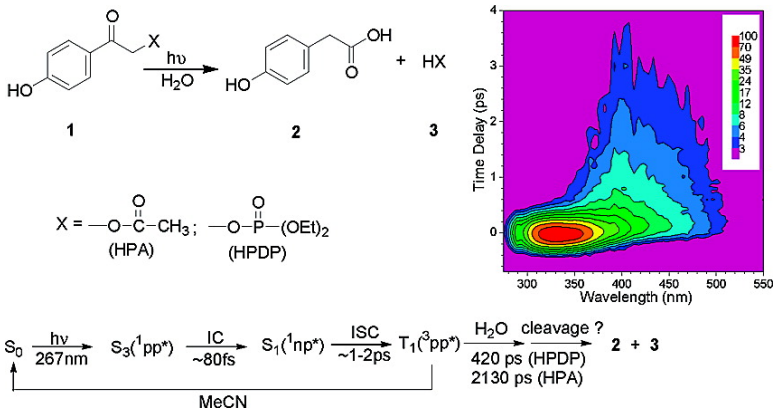

More About This Article

Additional resources and features associated with this article are available within the HTML version:

- Supporting Information
- Links to the 13 articles that cite this article, as of the time of this article download
- Access to high resolution figures
- Links to articles and content related to this article
- Copyright permission to reproduce figures and/or text from this article

View the Full Text HTML

J|A|C|S
ARTICLES
Published on Web 01/12/2005

Ultrafast Time-Resolved Study of Photophysical Processes Involved in the Photodeprotection of *p*-Hydroxyphenacyl Caged Phototrigger Compounds

Chensheng Ma, Wai Ming Kwok, Wing Sum Chan, Peng Zuo, Jovi Tze Wai Kan, Patrick H. Toy, and David Lee Phillips*

Contribution from the Department of Chemistry, The University of Hong Kong, Pokfulam Road, Hong Kong S.A.R., P. R. China

Received July 10, 2004; E-mail: phillips@hkucc.hku.hk

Abstract: A combined femtosecond Kerr gated time-resolved fluorescence (fs-KTRF) and picosecond Kerr gated time-resolved resonance Raman (ps-KTR^3) study is reported for two *p*-hydroxyphenacyl (*p*HP) caged phototriggers, HPDP and HPA, in neat acetonitrile and water/acetonitrile (1:1 by volume) solvents. Fs-KTRF spectroscopy was employed to characterize the spectral properties and dynamics of the singlet excited states, and the ps-KTR^3 was used to monitor the formation and subsequent reaction of triplet state. These results provide important evidence for elucidation of the initial steps for the *p*HP deprotection mechanism. An improved fs-KTRF setup was developed to extend its detectable spectral range down to the 270 nm UV region while still covering the visible region up to 600 nm. This combined with the advantage of KTRF in directly monitoring the temporal evolution of the overall fluorescence profile enables the first time-resolved observation of dual fluorescence for *p*HP phototriggers upon 267 nm excitation. The two emitting components were assigned to originate from the $^1\pi\pi^*$ (S_3) and $^1n\pi^*$ (S_1) states, respectively. This was based on the lifetime, the spectral location, and how these varied with the type of solvent. By correlating the dynamics of the singlet decay with the triplet formation, a direct $^1n\pi^* \rightarrow {}^3\pi\pi^*$ ISC mechanism was found for these compounds with the ISC rate estimated to be $\sim 5 \times 10^{11}$ s^{-1} in both solvent systems. These photophysical processes were found to be little affected by the kind of leaving group indicating the common local *p*HP chromophore is largely responsible for the fluorescence and relevant deactivation processes. The triplet lifetime was found to be ~420 and 2130 ps for HPDP and HPA, respectively, in the mixed solvent compared to 150 and 137 ns, respectively, in neat MeCN. The solvent and leaving group dependent quenching of the triplet is believed to be associated with the *p*HP deprotection photochemistry and indicates that the triplet is the reactive precursor for *p*HP photorelease reactions for the compounds examined in this study.

Introduction

Rapid and localized liberation of biological stimulants is needed for real-time monitoring of physiological responses in biological systems.[1−7] The *p*-hydroxyphenacyl (*p*HP) group was recently found to be such an efficient "cage" for the photorelease of various biological functional groups.[8−10] Photodeprotection of *p*HP phototriggers occur exclusively in aqueous or aqueous containing media. However, in pure organic solvents such as acetonitrile (MeCN), photoexcitation leads solely to photophysical processes resulting in the recovery of the corresponding ground state molecule. The products of the deprotection are well established, but much uncertainty exists about the events that lead to their formation. An example of the products produced from the deprotection of two *p*HP compounds are shown below:

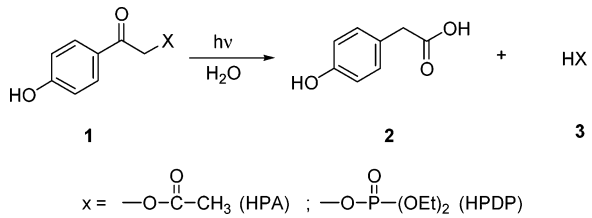

Previous mechanistic studies indicate a series of fast steps are involved in the *p*HP deprotection.[11−13] However, there are

(1) Givens, R. S.; Kueper, L. W. *Chem. Rev.* **1993**, *93*, 55−66 and references therein.
(2) Givens, R. S.; Athey, P. S.; Matuszewski, B.; Kueper, L. W., III.; Xue, J. Y.; Fister, T. *J. Am. Chem. Soc.* **1993**, *115*, 6001−6012 and references therein.
(3) (a) Givens, R. S.; Athey, P. S.; Kueper, L. W., III; Matuszewski, B.; Xue, J.-Y. *J. Am. Chem. Soc.* **1992**, *114*, 8708−8710. (b) Gee, K. R.; Kueper, L. W., III; Barnes, J.; Dudley, G.; Givens, R. S. *J. Org. Chem.* **1996**, *61*, 1228−1233.
(4) (a) Il'ichev, Y. V.; Schworer, M. A.; Wirz, J. *J. Am. Chem. Soc.* **2004**, *126*, 4581−4595. (b)Rajesh, C. S.; Givens, R. S.; Wirz, J. *J. Am. Chem. Soc.* **2000**, *122*, 611−618. (c) Hangarter, M.-A.; Hörmann, A.; Kamdzhilov, Y.; Wirz, J. *Photochem. Photobiol. Sci.* **2003**, *2*, 524−535.
(5) Rock, R. S.; Chan, S. I. *J. Am. Chem. Soc.* **1998**, *120*, 10766−10767.
(6) Namiki, S.; Arai, T.; Rujimori, K. *J. Am. Chem. Soc.* **1997**, *119*, 3840−3841.
(7) (a) Lee, K.; Falvey, D. E. *J. Am. Chem. Soc.* **2000**, *122*, 9361−9366. (b) Banerjee, A.; Lee, K.; Yu, Q.; Fan, A. G.; Falvey, D. E. *Tetrahedron lett.* **1998**, *39*, 4635−4638. (c) Banerjee, A.; Falvey, D. E. *J. Org. Chem.* **1997**, *62*, 6245−6251.
(8) Givens, R. S.; Weber, J. F. W.; Conrad, P. G., II; Orosz, G.; Donahue, S. L.; Thayer, S. A. *J. Am. Chem. Soc.* **2000**, *122*, 2687−2697 and references therein.
(9) Conrad, P. G., II; Givens, R. S.; Weber, J. F. W.; Kandler, K. *Org. Lett.* **2000**, *2*, 1545−1547.

conflicting interpretations of these processes and the actual identity of the putative intermediates involved in the deprotection reaction. The different interpretations are mainly focused on the issue of the multiplicity for the reactive precursor and the mechanism for the cleavage step in the overall reaction. Givens et al. identified a short-lived triplet as the precursor for *p*HP diethyl phosphate (HPDP) and favored a direct triplet cleavage pathway for the phosphate release.[8−11] Wan et al. reported a singlet mechanism for *p*HP acetate (HPA) and proposed that the primary event for the photochemistry is the singlet excited-state intramolecular proton transfer (ESIPT) mediated by water solvent molecules.[12] Information regarding the intersystem crossing (ISC) process and its solvent dependence (neat MeCN vs H_2O/MeCN mixed solvent) is crucial to resolving the controversy about the multiplicity of the reactive precursor intermediate. In addition, knowledge of the dynamics for event-(s) that take place due to the presence of H_2O in the solvent environment and the possible influence on the dynamics by different leaving groups is essential to understand the cleavage mechanism for the deprotection reactions. Time-resolved measurements are needed to provide direct experimental evidence for the photophysical processes and reactive intermediates involved in the deprotection reactions. To help address this, transient absorption experiments with nanosecond and picosecond time-resolution have been reported for HPA[12] and HPDP,[11] respectively. Although valuable information has been derived from these studies, there are still several important gaps that need to be addressed such as the initial photophysical events and unambiguous evidence for the multiplicity of the reactive precursor intermediate that reacts with water.

In this report, femtosecond Kerr gated time-resolved fluorescence (fs-KTRF) combined with picosecond Kerr gated time-resolved resonance Raman (ps-KTR[3]) spectroscopy have been employed for both HPA and HPDP in neat MeCN and H_2O/MeCN mixed solvent systems. The spectral properties and rapid decay of the singlet excited states were characterized by the fs-KTRF measurements, and the generation and fate of the triplet state were monitored by the ps-KTR[3] experiments.

HPA and HPDP belong to aromatic carbonyl compound that have been long known to have very small fluorescence yields predominately due to ISC conversion that quickly deactivates the singlet state(s).[14−20] Because of experimental difficulties associated with the extremely short singlet lifetime, weak fluorescence, and the location of the fluorescence profile in the UV region, there has been no solution phase time-resolved fluorescence work reported for this class of compounds to our knowledge. To deal with the problems associated with obtaining ultrafast fluorescence spectra in the UV region, we have recently developed an improved fs-KTRF system to extend the detectable spectral range down to 270 nm in the UV region and still cover the visible region up to 600 nm. With the advantage of the KTRF being able to directly monitor the temporal evolution of the overall fluorescence profile,[21,22] dual fluorescence has been observed for the first time for the *p*HP class of compounds. Assignment of the emitting states has been made based on their temporal evolution and the dependence of their spectral properties on solvent.

Picosecond-KTR[3] technique has been used for the triplet Raman measurements. By correlating the singlet decay times from the fs-KTRF spectra with the triplet formation time from the ps-KTR[3] spectra, the ISC mechanism has been determined and the ISC rate was estimated. To evaluate the crucial role of water for the deprotection reaction to take place, we compared the femtosecond to nanosecond dynamics for HPA and HPDP in neat MeCN vs H_2O/MeCN mixed solvents. These results provide strong evidence for the multiplicity of the intermediate that is predominantly produced and further reacts with water in the deprotection reaction. The present results also shed additional light on the initial photophysical steps involved in the deprotection mechanism of the *p*HP class of phototrigger compounds.

Experimental Methods

Preparation of HPA and HPDP Samples. HPA was synthesized following the methods given in refs 12, 23, and 24, and the synthesis of HPDP is described in the Supporting Information. The identity and purity of the samples were confirmed by analysis of MS, NMR, and UV absorption spectroscopy. The details of the synthesis and characterization of HPA and HPDP are given in the Supporting Information. Spectroscopic grade acetonitrile (MeCN), methanol (MeOH), and tetrahydrofuran (THF) as well as deionized water were used as solvents for the experiments.

Femtosecond Kerr Gated Time-Resolved Fluorescence (fs-KTRF) Experiments. Third harmonic (267 nm) and fundamental laser pulses (800 nm) from a commercial Ti:Sapphire regenerative amplifier laser system with a 150 fs pulse duration and 1 kHz repetition rate were used as excitation and gating pulses, respectively, for the fs-KTRF experiments. The excitation pulses (~0.5 μJ) were focused (~100 μm) into a 0.5 mm thickness jet stream of sample placed at one focus of an elliptical mirror. The emission from the sample was collected by the elliptical mirror and passed through a film polarizer then focused into the Kerr medium (a 1 mm thickness fused silica plate) placed at the other focus point of the ellipse. The Kerr medium was placed between a crossed polarizers pair with an extinction ratio of ~10^4. The gating beam was polarized at 45° and focused to the Kerr medium with adjusted intensity to create, in effect, a half-waveplate that rotates the polarization of the light from the sample allowing it to be transmitted through a Glan Taylor polarizer for the duration of the induced anisotropy created by the femtosecond gating pulse. The emission that passed through the second polarizer was focused into a monochromator and detected by a liquid nitrogen cooled CCD detector. The fluorescence measurement was performed at the magic angle to eliminate the effect of sample reorientation. The Kerr gate was opened to sample the

(10) (a) Gives, R. S.; Park, C.-H. *Tetrahedron Lett.* **1996**, *37*, 6259−6262. (b) Park, C.-H.; Givens, R. S. *J. Am. Chem. Soc.* **1997**, *119*, 2453−2463. (c) Givens, R. S.; Jung, A.; Park, C.-H.; Weber, J.; Bartlett, W. *J. Am. Chem. Soc.* **1997**, *119*, 8369−8370.
(11) Conrad, P. G., II; Givens, R. S.; Hellrung, B.; Rajesh, C. S.; Ramseier, M.; Wirz, J. *J. Am. Chem. Soc.* **2000**, *122*, 9346−9347.
(12) (a) Zhang, K.; Corrie, J. E. T.; Munasinghe, V. R. N.; Wan, P. *J. Am. Chem. Soc.* **1999**, *121*, 5625−5632. (b) Brousmiche, D. W.; Wan, P. *J. Photochem. Photobiol., A* **2000**, *130*, 113−118.
(13) Banerjee, A.; Falvey, D. E. *J. Am. Chem. Soc.* **1998**, *120*, 2965−2966.
(14) Ohshima, Y.; Fujii, T.; Fujita, T.; Inaba, D.; Baba, M. *J. Phys. Chem. A* **2003**, *107*, 8851−8855.
(15) Baronavski, A. P.; Owrutsky, J. C. *Chem. Phys. Lett.* **2001**, *333*, 36−40.
(16) (a) Ohmori, N.; Suzuki, T.; Ito, M. *J. Phys. Chem.* **1988**, *92*, 1086−1093. (b) Kamei, S.; Okuyama, K.; Abe, H.; Mikami, N.; Ito, M. *J. Phys. Chem.* **1986**, *90*, 93−100.
(17) Greene, B. I.; Hochstrasser, R. M.; Weisman, R. B. *J. Chem. Phys.* **1979**, *70*, 1247−1259.
(18) Damschen, D. E.; Merritt, C. D.; Perry, D. L.; Scott, G. W.; Talley, L. D. *J. Phys. Chem.* **1978**, *82*, 2268−2272.
(19) Rentzepis, P. M. *Science* **1970**, *169*, 239−247.
(20) Li. R.; Lim, E. C. *J. Chem. Phys.* **1972**, *57*, 605−612.
(21) Browne, W. R.; Coates, C. G..; Brady, C.; Matousek, P.; Towrie, M.; Botchway, S. W.; Parker, A. W.; Vos, J. G.; McGarvey, J. J. *J. Am. Chem. Soc.* **2003**, *125*, 1706−1707.
(22) Kwok, W. M.; Ma, C.; Matousek, P.; Parker, A. W.; Phillips, D.; Towrie, M. *J. Phys. Chem. A* **2000**, *104*, 4188−4197 and reference therein.
(23) Kihara, M.; Ikeuchi, I.; Kobayashi, Y.; Nagao, Y.; Hashizume, M.; Moritoki, H. *Drug Des. Discovery* **1994**, *11*, 175−183.
(24) Banerjee, A.; Lee, K.; Falvey, D. E. *Tetrahedron* **1999**, *55*, 12699−12710.

fluorescence spectrum at various time delays following the excitation pulse by employing a computer controlled optical delay line. All KTRF spectra were obtained by subtracting the negative time delay signal from the positive time delay signal and corrected for the detection system transmission/sensitivity variation with wavelength and the wavelength-dependent time shift due to the group velocity dispersion (GVD). The wavelength sensitivity variation correction curve was obtained by comparing the 20 ps time delay KTRF spectrum of trans-stilbene (this covers the spectral range of interest in the present study and shows very little change on the shape of the KTRF spectra at difference time delays) with its sensitivity corrected steady-state spectrum from a commercial fluorescence spectrometer. The GVD of the system (which was about 400 fs from 280 to 500 nm) was corrected by equation $\delta t = 0.0033\lambda^2 - 4.5117\lambda + 1253.8$, where δt is time shift (fs) and λ is wavelength (nm). The constants are estimated by peak fitting of the KTRF spectra of white light continuum created by intense pump pulse. The instrument response functions (IRF), which are wavelength dependent and vary from 200 to 350 fs for wavelength 500 to 280 nm, were measured from the duration of the white light continuum and also the fluorescence rise time from trans-stilbene.

Picosecond Kerr Gated Time-Resolved Resonance Raman (ps-KTR^3) Experiments. For the ps-KTR^3 measurements, the Ti:Sapphire regenerative amplifier laser system was operated in picosecond mode with a 800 nm, ~1 ps, and 1 kHz output. Samples were pumped by 267 nm pulse and probed with 400 and 342 nm pulses. The 267 nm pump and 400 nm probe pulses were the third and second harmonic of the regenerative amplifier fundamental, respectively. The 342 nm probe pulse was generated by mixing of the 800 nm pulse and the 532 nm output from a home-built OPA system pumped by the 400 nm laser pulse. The pump and probe pulse durations were ~1.5 ps; the pulse energies at the sample were 2−3 μJ. The sampling and signal collecting systems were the same as those in the fs-KTRF experiments except that the film polarizer was replaced by a Glan Taylor polarizer and the Kerr medium was changed to a 2 mm UV cell with benzene in it to improve the extinction ratio and efficiency of the gate. The polarization of the pump and probe beams were set at the magic angle and focused to a spot size of approximately 200 μm at the sample. Details of the ps-KTR^3 experimental apparatus our laser system is based on are given in refs 25 and 26.

The fs-KTRF and ps-KTR^3 spectra were calibrated by using Hg lamp and solvent Raman peaks, respectively. Sample solutions for these experiments were typically at ~1 mM concentration and renewed every 2 hours during the experiments, and within this period of time no degradation was observed by UV absorption spectroscopy.

Results and Discussion

A. Femtosecond Kerr Gated Time-Resolved Fluorescence (fs-KTRF) Spectroscopy. Figure 1a shows the 3D contour of the KTRF spectra for HPA obtained with 267 nm excitation in MeCN with a time delay up to 4 ps after excitation. Clearly, rather than a simple decay of one band, the fluorescence profile shows two components in both the time and wavelength regimes. An intense emission band with a maximum near 340 nm predominates at very early times and disappears at ~0.5 ps. The relatively weak emission band that has a maximum at ~420 nm persists up to ~3 ps. Fluorescence decay kinetics at 330 and 440 nm together with the IRF are displayed in Figure 1b. The IRF is represented by a Gaussian band shape with a 290 fs at 330 nm.

It is also shown in Figure 1b that, by convolution with the IRF, both the decay curves can be simulated satisfactorily by a sum of two exponential components with time constants of 0.08 and 1.78 ps, respectively, but employing different proportionality factors. The 330 nm decay is predominantly by the faster component, while the longer-lived component contributes mostly to the decay of the 440 nm emission band. Decay kinetics at other wavelengths can be fitted in the same way. This appears to indicate that the fluorescence is composed of two components originating from different electronic excited states. Provided the different lifetimes, we tentatively take the spectrum recorded at −0.2 and 0.9 ps (shown in Figure 1c) as representative of the net fluorescence spectrum for the short- and long-lived emissive states, respectively. According to the spectral location, they are denoted temporarily to "blue" and "red" fluorescence, respectively. We found that, by using a log-normal function[27]

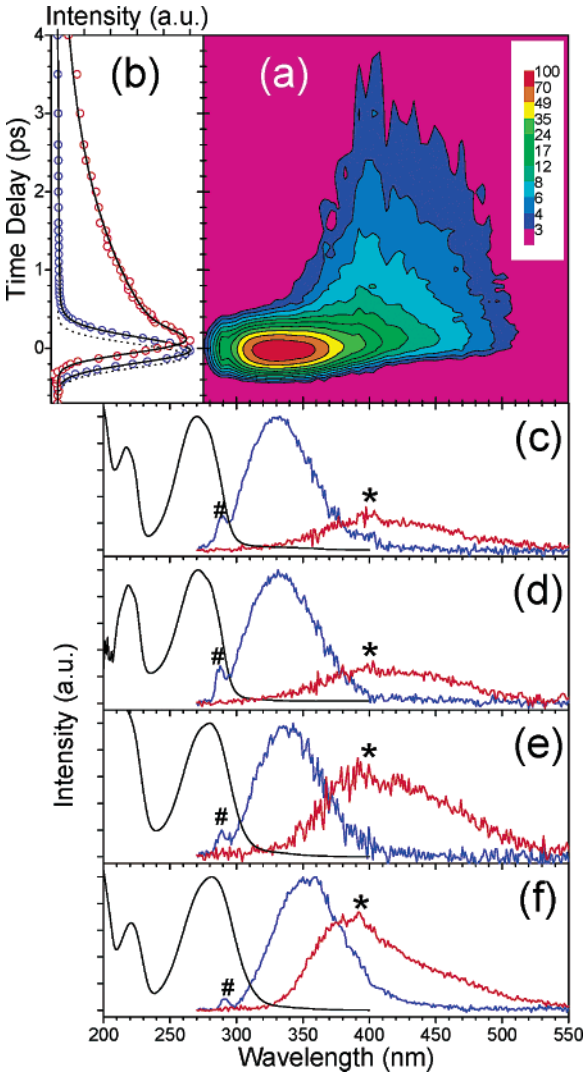

Figure 1. (a) Kerr gated time-resolved fluorescence contour of HPA (*p*-hydroxyphenacyl acetate) obtained with 267 nm excitation in MeCN. (b) Normalized fluorescence decay at 330 nm (circles in blue) and 440 nm (circles in red) for HPA in MeCN. The solid lines show two exponential fittings to the experimental data; the dotted line is the instrumental response function (see text for details). (c−f) Steady-state absorption spectrum (in black) and typical fluorescence profile of the blue (in blue) and red (in red) fluorescence for HPA in MeCN (c), THF (d), MeOH (e), and 90% H_2O/10% MeCN mixed solvent (f). The absorption spectra were normalized to the blue fluorescence spectra. Sharp features indicated by "#" and "*" are the solvent Raman band and the second harmonic generation of the 800 nm gating pulse from the Kerr medium, respectively.

(25) Matousek, P.; Towrie, M.; Ma, C.; Kwok, W. M.; Phillips, D.; Toner, W. T.; Parker, A. W. *J. Raman Spectrosc.* **2001**, *32*, 983−988.
(26) Matousek, P.; Towrie, M.; Stanley, A.; Parker, A. W. *Appl. Spectrosc.* **1999**, *53*, 1485−1489.

Table 1. Kerr Gated Time-Resolved Fluorescence and Steady-State Absorption Spectral Parameters for HPA and HPDP in Neat and 90% H_2O/10% MeCN (v/v) Mixed Solvents

	HPA				HPDP	
	MeCN	90%H_2O	MeOH	THF	MeCN	90%H_2O
τ_1 (ps)	0.08 ± 0.03	0.08 ± 0.03	0.08 ± 0.03	0.11 ± 0.03	0.08 ± 0.03	0.07 ± 0.03
τ_2 (ps)	1.78 ± 0.05	0.89 ± 0.05	1.25 ± 0.05	1.90 ± 0.05	1.98 ± 0.05	0.76 ± 0.05
λ_1^{fluo} (nm)	334	356	341	334	331	354
λ_2^{fluo} (nm)	427	392	420	433	433	401
λ^{abs} (nm)	272	280	279	273	273	280
ϵ ($\times 10^4$ L mol^{-1} cm^{-1})	1.45	1.23	1.35	1.42	1.28	0.86
I_2/I_1 ($\times 10^{-2}$)	4.4	16	6.9	5.4	6.1	15
Φ ($\times 10^{-5}$)	5.0	6.5	5.5	7.3	5.5	4.0

(see Supporting Information for details) and nonlinear least-squares regression, the fluorescence profile obtained at each time delay can be reproduced by overlap of the blue and red components with different weighted factors. The weaker intensity of the red band compared to the blue band may reflect the weaker oscillator strength of the former than latter transition.

The resemblance of the steady-state absorption spectra of HPA and HPDP to that of the "cage" *p*-hydroxyacetophenone (HA) (see Supporting Information for the comparative absorption spectra) indicates that, for both of the compounds, the *p*HP moiety is the chromophore responsible for the photoexcitation. The 267 nm photoexcitation of these compounds leads to the prompt population of the strongly allowed $\pi\pi^*$ (L_a type) S_3 state associated with the lowest strong absorption band (shown in Figure 1c). The two lower energy $\pi\pi^*$ S_2 (L_b type) and nπ^* S_1 bands are buried under the intense S_3 band due to their closeness (the S_2 state) to the S_3 absorption and their weaker oscillator strength (both the S_1 and S_2 states).[28−30] The S_1 absorption was found to be at ∼346 nm for HA.[29] Extensive investigations on aromatic carbonyl compounds reveal that the energy levels of the excited $\pi\pi^*$ and nπ^* states are affected significantly by the solvent H-bonding strength and the solvent polarity: increasing the H-bonding strength or polarity stabilizes the $\pi\pi^*$ states, whereas these effects destabilize the nπ^* state at the same time.[31−39] This solvent-dependent modification of these energy levels has been well rationalized and ascribed to account for the characteristic blue shift of the nπ^* and red shift of the $\pi\pi^*$ spectral bands in solution.[31−33,40,41] It is therefore necessary to perform the KTRF measurement in solvents of different polarity and H-bonding ability to help assign the observed fluorescence and to justify the above dual fluorescence assignment. In addition to neat MeCN that is an aprotic solvent with high polarity (ϵ = 33.8) and 90% H_2O/10% MeCN (v/v) mixed solvent that is a strong H-bonding and very polar solvent, we chose two additional solvents methanol (MeOH) and tetrahydrofuran (THF) for KTRF experiments on HPA. MeOH has a midrange H-bonding strength and a polarity (ϵ = 33.1) similar to that of MeCN, while THF is an aprotic solvent of weak polarity (ϵ = 7.6).[27,41]

The KTRF results obtained in the H_2O/MeCN mixed solvent, MeOH, and THF are generally similar to that in pure MeCN but with distinct variations in the spectral location and decay rate in the different solvents. Table 1 lists the time constants obtained from fitting the 330 and 440 nm decay kinetics in the four different solvents. The maximum band positions of the typical blue and red fluorescence bands and the corresponding steady-state S_3 absorption band are also summarized in Table 1. The band positions were acquired by log-normal fitting of the respective spectral profile (see Supporting Information). In Figure 1d−f, the typical fluorescence and absorption spectra in THF, MeOH, and H_2O/MeCN mixed solvent are shown respectively to compare with those recorded in pure MeCN.

From Table 1 and Figure 1c−f, it is clear that, from MeCN to MeOH to H_2O/MeCN mixed solvent, the blue fluorescence downshifts to the red and the red fluorescence upshifts to the blue. These changes in the spectral location are accompanied by a lifetime shortening of the red band and an increase in the intensity ratio of the red to blue band manifested by I_2/I_1 in Table 1 (see Supporting Information for how these were estimated). The THF data are rather close to those of MeCN but with a slight red shift and longer lifetime for the THF red band compared to that of MeCN. Obviously, the solvent H-bonding and polarity dependent shifts coincide with the characteristic solvent-dependent spectral shift expected for these aromatic compounds. We consider this as convincing evidence for the coexistence of two fluorescence components; one is the $\pi\pi^*$ character state emitting the blue fluorescence, and the other is the nπ^* state emitting the red fluorescence. We note that processes such as excited-state intramolecular vibrational redistribution (IVR), vibrational relaxation, and solvent reorientation can lead to spectral shifts and bandwidth changes for TRF profiles and may sometimes occur in similar time scales.[27,42−44] Although some of these processes could possibly occur for

(27) Horng, M. L.; Gardecki, J. A.; Papazyan, A.; Maroncelli, M. *J. Phys. Chem.* **1995**, *99*, 17311−17337.
(28) Dym, S.; Hochstrasser, R. M. *J. Chem. Phys.* **1969**, *51*, 2458−2468.
(29) (a) Kearns, D. R.; Case, W. A. *J. Am. Chem. Soc.* **1966**, *88*, 5087−5097. (b) Case, W. A.; Kearns, D. R. *J. Chem. Phys.* **1970**, *52*, 2175−2191.
(30) Chan, W. S.; Ma, C.; Kwok, W. M.; Zuo, P.; Phillips, D. L. *J. Phys. Chem. A* **2004**, *108*, 4047−4058.
(31) (a) Bhasikuttan, A. C.; Singh, A. K.; Palit, D. K.; Sapre, A. V.; Mittal, J. P. *J. Phys. Chem. A.* **1998**, *102*, 3470−3480. (b) Singh, A. K.; Bhasikuttan, A. C.; Palit, D. K.; Mittal, J. P. *J. Phys. Chem. A* **2000**, *104*, 7002−7009.
(32) (a) Mitsui, M.; Ohshima, Y. *J. Phys. Chem. A* **2000**, *104*, 8638−8648. (b) Mitsui, M.; Ohshima, Y.; Ishiuchi, S.-i.; Sakai, M.; Fujii, M. *J. Phys. Chem. A* **2000**, *104*, 8649−8659. (c) Mitsui, M.; Ohshima, Y.; Kajimoto, O. *J. Phys. Chem. A* **2000**, *104*, 8660−8670.
(33) (a) Morlet-Savary, F.; Ley, C.; Jacques, P.; Wieder, F.; Fouassier, J. P. *J. Photochem. Photobiol. A.* **1999**, *126*, 7−14. (b) Ley, C.; Morlet-Savary, F.; Jacques, P.; Fouassier, J. P. *Chem. Phys.* **2000**, *255*, 335−346.
(34) Cavaleri, J. J.; Prater, K.; Bowman, R. M. *Chem. Phys. Lett.* **1996**, *259*, 495−502.
(35) van der Burgt, M. J.; Jansen, L. M. G.; Huizer, A. H.; Varma, C. A. G. O. *Chem. Phys* **1995**, *201*, 525−538.
(36) Hamanoue, K.; Nakayama, T.; Yamaguchi, T.; Ushida, K. *J. Phys. Chem.* **1989**, *93*, 3814−3818.
(37) Scaiano, J. C. *J. Am. Chem. Soc.* **1980**, *102*, 7747−7753.
(38) Dalton, J. C.; Montgomery, F. C. *J. Am. Chem. Soc.* **1974**, *96*, 6230−6232.
(39) Rusakowicz, R.; Byers, G. W.; Leermakers, P. A. *J. Am. Chem. Soc.* **1971**, *93*, 3263−3266.
(40) Turro, N. J. *Modern Molecular Photochemistry*; University Science Book: California, 1991.
(41) Reichardt, C. *Solvent and Solvent Effect in Organic Chemistry*; VCH: Verlagsgesellschaft mbH, D-6940 Weinheim, 1988.
(42) Macpherson, A. N.; Gillbro, T. *J. Phys. Chem. A* **1998**, *102*, 5049−5058.

photoexited HPA, the specific solvent-dependent lifetime and spectral shifts indicate that none of them are likely to be the major factor accounting for the KTRF observations.

Consistent with the $\pi\pi^*$ nature of the S_3 state, the S_3 absorption band shifts to the red from MeCN/THF to MeOH to H_2O/MeCN mixed solvent (Table 1), and this behavior parallels the observed shifts of blue fluorescence band. This combined with the allowed nature of the relatively intense blue fluorescence band and the roughly mirror image between it and the S_3 $\pi\pi^*$ absorption band leads us to assign the S_3 state as the source emitting the blue fluorescence. The weakness of the red fluorescence is consistent with its origin from the weakly allowed S_1 $n\pi^*$ state. According to these assignments and using the $^1\pi\pi^*$ (S_3) extinction coefficient (the ϵ values listed in Table 1) deduced from the absorption spectra,[40,45] an overall fluorescence yield of $\sim 6 \times 10^{-5}$ (this does not much depend on the solvent system) can be estimated based on the integration of the measured KTRF spectra and the fluorescence lifetimes (Table 1; for details see Supporting Information).[46] This is consistent with previous observations that the fluorescence of HA is below the normal steady-state detection limit and indicates a very high efficiency of the singlet deactivation processes.[20]

We note the possibility of interference from the L_b type $\pi\pi^*$ S_2 state to the blue fluorescence. The S_0 to S_2 transition is symmetrically forbidden but the L_b state can mix with the nearby L_a $\pi\pi^*$ (S_3) state by vibrational coupling and borrow intensity from the optically allowed S_3 state.[28−30,47] However, based on the result that the KTRF decay kinetics can be fitted reasonably well by only two exponential components, we consider the blue fluorescence is predominantly from the S_3 state in this preliminary account and the S_2 state will not be considered further here. To avoid any ambiguity in the assignments, we refer hereafter to the emitting states to be $^1\pi\pi^*$ and $^1n\pi^*$, rather than S_3 and S_1, as the origin of the blue and red fluorescence bands, respectively.

The KTRF results for HPDP in MeCN and 90% H_2O/10% MeCN mixed solvent are similar to those of HPA in the corresponding solvents and the data obtained is also listed in Table 1. In addition, for both HPA and HPDP, the KTRF spectra in 50% H_2O/50% MeCN (v:v) mixed solvent were found to be almost identical to the corresponding spectra recorded in 90% H_2O/10% MeCN mixed solvent. The similarity between the KTRF spectra of HPA and HPDP implies the properties of the emitting states are little affected by the leaving group consistent with the *p*HP subgroup being the common chromophore for the fluorescence processes.

The moderate solvent polarity dependence and small Stokes shift between the $^1\pi\pi^*$ absorption (S_3) and the fluorescence bands imply the $^1\pi\pi^*$ state has little charge transfer (CT) character consistent with the previously reported L_a $^1\pi\pi^*$ character for aromatic carbonyl compounds with hydroxy substitution at the *para*-position.[31,48] On the other hand, the observation that the extent of the fluorescence shifts (for both $^1\pi\pi^*$ and $^1n\pi^*$) correlates with the solvent H-bonding strength indicates the importance of excited state solvent−solute H-bonding interaction in affecting the $\pi^* \rightarrow \pi$ and $\pi^* \rightarrow n$ emission processes. From Table 1, it can be seen that, due to the H-bonding interaction, the energy separation between the emitting $^1\pi\pi^*$ and $^1n\pi^*$ states reduces substantially from $\sim$6500 cm^{-1} in neat MeCN to $\sim$2600 cm^{-1} in H_2O/MeCN mixed solvent for HPA and a similar amount for HPDP. This consequently results in stronger vibronic coupling between the two states in H_2O/MeCN mixed solvent than in neat MeCN solvent. Out-of-plane vibrations such as $-C(O)CH_2-$ torsion and $-(O)C-CH_2-$ rotation could be the most probable modes to effectively couple these two states.[49] This vibronic coupling between the close-lying $^1\pi\pi^*$ and $^1n\pi^*$ states, the so-termed "proximity effect", influences substantially the radiative and nonradiative dynamics of the excited states and can account for the lifetime and additional spectral differences observed here in aprotic vs protic solvents (see below).[35,50] We note, however, that the order of the $\pi\pi^*$ vs $n\pi^*$ energy level remains the same in all the solvents investigated. This implies that deactivation processes of the two singlet states will not be dramatically different in the two kinds of solvent, and this is indeed confirmed by the ISC dynamics revealed in the following ps-TR^3 experiments.

The dual fluorescence phenomenon was first reported for 4-dimethylaminobenzonitrile (DMABN) and its derivatives more than forty years ago.[22,51] The solvent polarity has been deduced as the main factor to influence the DMABN fluorescence profile rather than the H-bonding strength.[51−53] In nonpolar solvents, the DMABN fluorescence is "normal" and originates from a locally excited (LE) state. An additional deeply red shifted band appears in polar solvents, and this new band has been found to be from an intramolecular charge transfer (ICT) state produced from the LE state on a picosecond time scale.[22,52−54] Obviously, the dual fluorescence observed here for HPA and HPDP is different from that of the DMABN family of compounds due to fundamental differences in the nature of the emitting states as well as the behavior of the solvent dependence. Here the $^1n\pi^*$ state is formed by internal conversion (IC) from the initially populated $^1\pi\pi^*$. The IC dynamics cannot be resolved in this work due to spectral overlap between the $^1\pi\pi^*$ and $^1n\pi^*$ fluorescence profile and the $\sim$250 fs time resolution but is expected to correspond to the $^1\pi\pi^*$ decay that has a $\sim$80 fs time constant as shown in Table 1. We note that, by using an ultrafast TRF technique, fluorescence from singlet excited states higher than S_1 has been reported for several systems[46,55−56]

(43) Gustavsson, T.; Cassara, L.; Gulbinas, V.; Gurzadyan, G.; Mialocq, J.-C.; Pommeret, S.; Sorgius, M.; van der Meulen, P. *J. Phys. Chem. A* **1998**, *102*, 4229−4245.
(44) Akimoto, S.; Yamazaki, I.; Sakawa, T.; Mimuro, M. *J. Phys. Chem. A* **2002**, *106*, 2237−2243.
(45) Dalton J. C.; Turro, N. J. *J. Am. Chem. Soc.* **1971**, *93*, 3569−3570.
(46) Takeuchi, S.; Tahara, T. *J. Phys. Chem. A* **1997**, *101*, 3052−3060.
(47) Leopold, D. G.; Hemley, R. J.; Vaida, V *J. Chem. Phys.* **1981**, *75*, 4758−4769.
(48) Bhasikuttan, A. C.; Singh, A. K.; Palit, D. K.; Sapre, A. V.; Mittal, J. P. *J. Phys. Chem. A* **1999**, *103*, 4703−4711.
(49) (a) Lim, E. C.; Li, Y. H.; Li, R. *J. Chem. Phys.* **1970**, *53*, 2443−2448. (b) Li, Y. H.; Lim, E. C. *Chem. Phys. Lett.* **1970**, *7*, 15−18.
(50) (a) Lim, E. C. *J. Phys. Chem.* **1986**, *90*, 6770−6777. (b) Lai, T.-i.; Lim, E. C. *Chem. Phys. Lett.* **1980**, *73*, 244−248.
(51) Grabowski, Z. R.; Rotkiewicz, K.; Rettig, W. *Chem. Rev.* **2003**, *103*, 3899−4032.
(52) Kwok, W. M.; George, M. W.; Grills, D. C.; Ma, C.; Matousek, P.; Parker, A. W.; Phillips, D.; Toner, W. T.; Towrie, M. *Angew Chem., Int. Ed.* **2003**, *42*, 1826−1830.
(53) Kwok, W. M.; Ma, C.; George, M. W.; Grills, D. C.; Matousek, P.; Parker, A. W.; Phillips, D.; Toner, W. T.; Towrie, M. *Phys. Chem. Chem. Phys.* **2003**, *5*, 1043−1050.
(54) Kwok, W. M.; Ma, C.; Matousek, P.; Parker, A. W.; Phillips, D.; Toner, W. T.; Towrie, M.; Umapathy, S. *J. Phys. Chem. A* **2001**, *105*, 984−990.
(55) Bhasikuttan, A. C.; Sapre, A. V.; Okada, T. *J. Phys. Chem. A* **2004**, *107*, 3030−3035.
(56) Leupin, W.; Berens, S. J.; Magde, D. *J. Phys. Chem.* **1984**, *88*, 1376−1379.

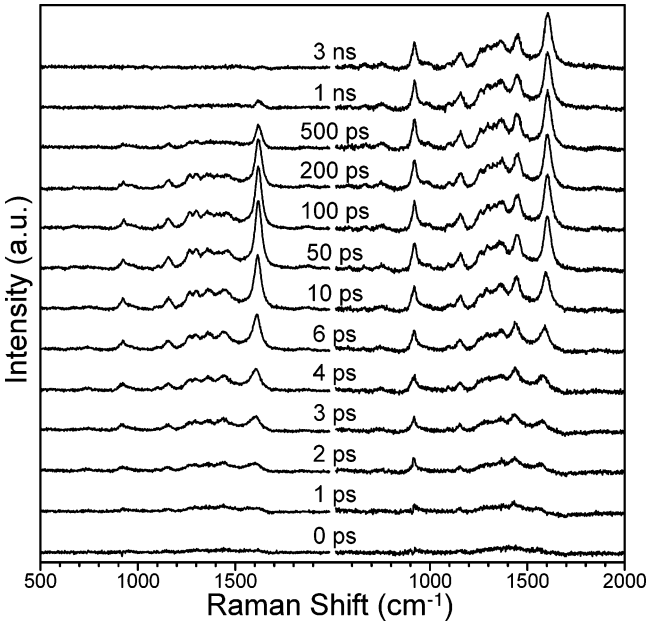

Figure 2. Picosecond Kerr gated time-resolved resonance Raman spectra of HPDP obtained with 267 nm pump and 400 nm probe wavelengths in 50% H_2O/50% MeCN mixed solvent (left) and neat MeCN (right).

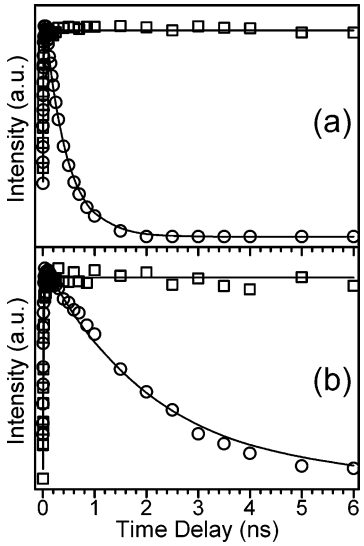

Figure 3. Temporal dependence of the triplet ~1600 cm^{-1} band areas for HPDP (a) and HPA (b) in 50% H_2O/50% MeCN mixed solvent (circles) and neat MeCN (squares) obtained in 400 nm probe ps-KTR^3 spectra. Solid lines show an exponential fitting of the experimental data.

including various carotenoids.[57−59] The observation here of the strong S_3 fluorescence is consistent with the large extinction coefficient of this $^1\pi\pi^*$ state vs the $^1n\pi^*$ S_1 state. It is worthwhile to point out that, to our knowledge, the fluorescence results presented here on HPA and HPDP represent the first ultrafast time-resolved fluorescence study on the *p*HP phototrigger compounds and also for related aromatic carbonyl compounds.

B. Picosecond Kerr Gated Time-Resolved Resonance Raman (ps-KTR^3) Spectroscopy. To establish the deactivation channel of the photopopulated $^1\pi\pi^*$ and $^1n\pi^*$ states, especially the ISC conversion to the triplet manifold, the dynamics for the triplet formation are essential to determine. Using a 267 nm pump and 400 nm probe excitation wavelengths, our recent TR^3 measurements found early picosecond formation and hundreds nanoseconds lifetime of the $\pi\pi^*$ triplet ($^3\pi\pi^*$) for HPA and HPDP in pure MeCN.[60,61] We performed the same experiments for the two compounds in 50% H_2O/50% MeCN (v/v) mixed solvent. Figure 2 displays the comparison between the spectra obtained in 50% H_2O/50% MeCN (v/v) mixed solvent to spectra obtained in neat MeCN for HPDP. Due to the 400 nm probe wavelength being near the maximum position of the $T_1 \rightarrow T_n$ absorption band[11] plus the similarity between the spectra in the two solvents, the spectra in the H_2O/MeCN mixed solvent can be attributed confidently to the HPDP $^3\pi\pi^*$ state. The corresponding ps-KTR^3 spectra for HPA are very similar to those of HPDP and are shown in the Supporting Information. As discussed in our earlier work,[60,61] the similarity of the triplet spectra of HPDP to those of HPA is indicative of the common chromophore (*p*HP moiety) and a similar triplet structure. For details of the vibrational spectra and assignments, the reader is referred to refs 60 and 61.

The temporal change of the Lorentzain fitted ~1600 cm^{-1} band area was found, and Figure 3a and b display a kinetic comparison for the $^3\pi\pi^*$ state in pure MeCN and H_2O/MeCN mixed solvent for HPDP and HPA, respectively. Clearly, the early time $^3\pi\pi^*$ development is similar for both the compounds in the two solvents (with ~7−12 ps time constant for the triplet growth); it is striking, however, that the $^3\pi\pi^*$ lifetime is much shorter in H_2O/MeCN mixed solvent than in pure MeCN solvent. The ~1600 cm^{-1} Raman band intensity decays were fitted using a single-exponential function, and lifetimes of 420 ± 10 ps and 2130 ± 10 ps were estimated for HPDP and HPA, respectively. The ~420 ps HPDP triplet decay time coincides with the ~400 ps time constant reported by Wirz and co-workers for the same system using transient absorption spectroscopy.[11] The triplet lifetime has been found to be ~150 and 137 ns for HPDP and HPA, respectively, in neat MeCN.[60,61] This solvent and leaving group dependent quenching of the triplet implies further reaction takes place on the triplet manifold specifically in the H_2O containing solvent. It is straightforward that the reaction is related to the *p*HP photocleavage process even if it does not directly undergo cleavage. We therefore ascribe the triplet decay time to the time scale occurring for the further deprotection photochemistry. The observations here are hence compelling evidence that the triplet state is the predominant reactive precursor to the *p*HP deprotection reaction and rules out the singlet mechanism[12] for HPA and HPDP after excitation with 267 nm light.

Since the ~7−12 ps growth time of the triplet does not exactly match the decay time of either the $^1\pi\pi^*$ or $^1n\pi^*$ fluorescence, further evidence is required to better elucidate the ISC mechanism. ps-KTR^3 spectra of HPA and HPDP obtained in pure MeCN and 50% H_2O/50% MeCN mixed solvents with 267 nm pump and 342 nm probe excitation wavelengths provide this needed information about the ISC mechanism. Figure 4a presents early time ps-KTR^3 spectra in the 1450−1800 cm^{-1}

(57) Holt, N. E.; Kennis, J. T. M.; Dall'Osto, L.; Bassi, R.; Fleming, G. R. *Chem. Phys. Lett.* **2003**, *379*, 305−313.
(58) Mimuro, M.; Nagashima, U.; Nagaoka, S.-i.; Nishimura, Y.; Takaichi, S.; Katoh, T.; Yamazaki, I. *Chem. Phys. Lett.* **1992**, *191*, 219−224.
(59) Kandori, H.; Sasabe, H.; Mimuro, M. *J. Am. Chem. Soc.* **1994**, *116*, 2671−2672.
(60) Ma, C.; Chan, W. S.; Kwok, W. M.; Zuo, P.; Phillips, D. L. *J. Phys. Chem. B* **2004**, *108*, 9264−9276.
(61) Ma, C.; Zuo, P.; Kwok, W. M.; Chan, W. S.; Kan, J. T. W.; Toy, P. H.; Phillips, D. L. *J. Org. Chem.* **2004**, *69*, 6641−6657.

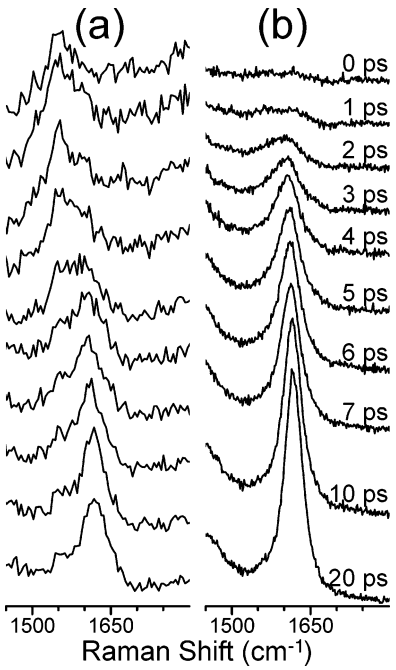

Figure 4. Picosecond Kerr gated time-resolved resonance Raman spectra obtained for HPDP in 50% H_2O/50% MeCN mixed solvent with 267 nm pump and 342 nm probe (a) and 400 nm probe (b) wavelengths, respectively.

region for HPDP in 50% H_2O/50% MeCN mixed solvent using 400 and 342 nm probe wavelengths after 267 nm pump excitation. It is clear that the band at ~1610 cm^{-1} appearing at 2 ps and afterward at both probe wavelengths is from the same $^3\pi\pi^*$ triplet that is also observed in spectra obtained in neat MeCN solvent (see Figure 2). Inspection of Figure 4 shows that an additional Raman band at about 1550 cm^{-1} appears only at very early times (up to 4 ps), and this feature decays very rapidly to form the $^3\pi\pi^*$ triplet state. The absence of the early time ~1550 cm^{-1} Raman band in the 400 nm probe ps-TR^3 spectra implies this 1550 cm^{-1} Raman band is from another short-lived species that is not the $^3\pi\pi^*$ triplet state. The lifetime of the species associated with the ~1550 cm^{-1} Raman band is within or close to the IRF of the present TR^3 system (~1−2 ps) and thus cannot be well-resolved but estimated to be on the same time-scale as the IRF. Similar spectra and dynamics were also observed for HPDP in neat MeCN solvent and for HPA in both solvent systems (these spectra are shown in the Supporting Information).

Significantly, the decay time of the early transient with the ~1550 cm^{-1} Raman band correlates with the lifetime of the red fluorescence attributed to the $^1n\pi^*$ S_1 state presented in the preceding KTRF measurements. Thus, we assign the new early time ~1550 cm^{-1} Raman band to be due to the $^1n\pi^*$ S_1 state. The appearance of the $^1n\pi^*$ Raman band in the 342 nm ps-KTR^3 spectra and its absence in the 400 nm ps-KTR^3 spectra implies the $^1n\pi^*$ $S_1 \rightarrow S_n$ transitions absorb appreciably at 342 nm but not at 400 nm. Previously reported transient absorption spectra indicate the 342 nm probe wavelength is located in the blue tail of the $T_1 \rightarrow T_n$ absorption for both HPA and HPDP in the two solvents.[11,12] This is consistent with the weaker Raman signal for the $^3\pi\pi^*$ triplet Raman bands in the 342 nm spectra compared to the 400 nm spectra. Probably due to the short S_1 lifetime, there has been very little $S_1 \rightarrow S_n$ transient absorption spectroscopy reported in the literature for the aromatic carbonyl family of molecules, and such information is not available for the *p*HP compounds studied here to the best of our knowledge. It would therefore be helpful at some point to acquire transient absorption spectra with femtosecond resolution in the future to directly observe the $S_1 \rightarrow S_n$ absorption and its spectral and kinetics evolution for these compounds.

C. ISC Mechanism and Deactivation of the Excited States. The dynamics and $^1n\pi^*$ S_1 assignment of the early species observed in the TR^3 spectra combined with the KTRF result indicates a direct $^1n\pi^*$ (S_1) → $^3\pi\pi^*$ (T_1) ISC pathway for the HPA and HPDP in neat and H_2O/MeCN mixed solvent. This may also suggest that such a mechanism is generally applicable for these compounds in other solvents. This ISC pathway is consistent with El-Sayed's rule and follows a direct spin−orbital coupling mechanism.[40] Givens and co-workers estimated the triplet energies of HPA and HPDP are 71.0 and 70.6 kcal/mol in EPA, corresponding in wavelength units to ~403 and 405 nm, respectively.[8] These values are rather close to the locations of the $^1n\pi^*$ fluorescence for the two compounds (Table 1) implying a small energy separation between the $^1n\pi^*$ and $^3\pi\pi^*$ level and consequent strong coupling between the two states. This provides an interpretation for the rapid ISC conversion and accounts for the short singlet lifetime and large triplet yield. This ISC mechanism associated with strong singlet−triplet coupling may be applicable generally to a wide range of aromatic carbonyls that have a lowest $n\pi^*$ singlet and $\pi\pi^*$ triplet, such as derivatives of acetophenone.

It is important to point out that our data provides no indication for the existence of an alternative ISC pathway $^1\pi\pi^*$ (S_3) → $^3n\pi^*$ (T_2) → $^3\pi\pi^*$ (T_1) although such a process is possible, since the T_2 state lies between the S_3 and T_1 and close to both the states.[29] Provided the ~80 fs S_3 lifetime (Table 1) and the fast T_2 to T_1 internal conversion that is believed to occur also in femtosecond time scale, the $^3\pi\pi^*$ state produced following this ISC channel can be expected to be detected promptly by our TR^3 measurements, which is not our experimental observation: as obviously indicated by the TR^3 spectra shown in Figures 2 and 4, the triplet is not detectable clearly until ~2 ps. It is therefore rather unlikely that this $^1\pi\pi^*$ (S_3) → $^3n\pi^*$ (T_2) → $^3\pi\pi^*$ (T_1) ISC pathway can account for the generation of the $^3\pi\pi^*$ studied here for HPA and HPDP.

Our result that the ISC occurs from the $^1n\pi^*$ S_1 state even with S_3 excitation has important implications in elucidating the deactivation processes of the excited states. It implies that (i) the major deactivation channel of the photopopulated S_3 state is internal conversion to S_1; (ii) the ISC of *p*HP caged compounds may be relatively independent of the excitation wavelength. We note that influence of excitation wavelength on ISC processes has been reported previously for some aromatic carbonyl compounds, and it appears that the effect can be especially significant under gas-phase conditions.[62−65] A kinetic model including ISC from both the $n\pi^*$ and $\pi\pi^*$ singlet states has also been proposed for aromatic carbonyl such as xanthone in solution phase.[34] On the other hand, Neckers, Rodgers, and co-workers reported very recently that the ISC of

(62) (a) Rennert, A. R.; Steel, C. *Chem. Phys. Lett.* **1981**, *78*, 36−39. (b) Berger, M.; Steel, C. *J. Am. Chem. Soc.* **1975**, *97*, 4817−4821.
(63) Itoh, T.; Baba, H.; Takemura, T. *Bull. Chem. Soc. Jpn.* **1978**, *51*, 2841−2846.
(64) Warren, J. A.; Bernstein, E. R. *J. Chem. Phys.* **1986**, *85*, 2365−2367.
(65) (a) Hirata, Y.; Lim, E. C. *J. Chem. Phys.* **1980**, *72*, 5505−5510. (b) Hirata, Y.; Lim, E. C. *J. Chem. Phys.* **1980**, *73*, 3804−3809.

benzophenone in solution is insensitive to the excitation wavelength.[66] This is consistent with our present results for HPA and HPDP in solution. Since the *p*HP deprotection reaction occurs on the triplet manifold, the independence of ISC process on excitation wavelength implies that the photorelease processes could also be relatively independent of the excitation wavelength. This may have some implication for practical applications of the *p*HP phototriggers in terms of selection of an excitation source. However, other factors also need to be considered. Compared with the S_1 excitation, using higher excitation energy (to S_2 or S_3) could possibly result in an enhanced efficiency of internal conversion back to ground state to deactivate the singlet excited state.[50,65] This could cause the triplet yield to be smaller with higher excitation than lower excitation energy. In this sense, the S_1 excitation with the wavelength above 300 nm, as generally employed in previous *p*HP deprotection studies,[8−12] would favor in giving high efficiency for liberation of the protected groups. Further work is needed to better address the actual wavelength dependence of the *p*HP deprotection reactions.

According to the $^1n\pi^*$ (S_1) → $^3\pi\pi^*$ (T_1) ISC pathway, estimation of the ISC rate requires, besides the $^1n\pi^*$ lifetime (Table 1), information of the $^1n\pi^* \rightarrow S_0$ internal conversion rate k_{IC}, that is not yet available for the compounds studied here to our knowledge. It has been well established in previous investigations that the relative contributions of IC vs ISC as nonradiative channels to deactivate the S_1 excited state are strongly influenced by the vibronic interaction between the close-lying $^1n\pi^*$ and $^1\pi\pi^*$ states that is, in turn, determined by the $^1n\pi^*$ and $^1\pi\pi^*$ energy gap: the smaller the energy gap, the stronger the vibronic coupling, and consequently the more efficient the IC process becomes to deactivate the S_1 state.[50,65] Based on this viewpoint, our result that the S_1 lifetime is shorter in H_2O/MeCN mixed solvent (~0.89 and 0.76 ps for HPA and HPDP, respectively, Table 1) than that in neat MeCN (~1.78 and 1.98 ps for HPA and HPDP, respectively, Table 1) combined with the much smaller $^1n\pi^*$ and $^1\pi\pi^*$ energy gap in the mixed than neat solvent might indicate an increased contribution of the IC to depopulate the S_1 state in the former rather than latter solvent. In this sense, the IC may not be negligible and competes with the ISC to deactivate the S_1 state. However, the generally high ISC yield as reported in previous work for aromatic carbonyl compounds[19,67] implies the predominance of the ISC as the deactivation channel. In addition, we note that phenols become more acidic in the excited than in the ground state; it is therefore necessary to consider the possibility that deprotonation of the phenolic proton could act as a competing process to deactivate the S_1 state. Previous work[9,11,12] found that the deprotonation does occur after photoexcitation of the *p*HP caged phototriggers but with a much slower rate, such as $\sim 9 \times 10^6$ s^{-1} for HA in 50% H_2O/50% MeCN (v/v),[11] than the decay of the S_1 state observed here. This combined with the fact that a similarly small fluorescence quantum yield and short singlet lifetime have been observed for several closely related aromatic compounds with the *para*-substitution with moieties other than the hydroxy group[19,67] (for example the methoxy[1,2,11,67] group) where the proton is not available implies that the deprotonation is not likely to account for the S_1 deactivation. However, as discussed below, deprotonation on the other hand could be involved in the deactivation of the triplet in aqueous solution. We therefore suggest the ISC rate as being $\sim 5 \times 10^{11}$ s^{-1} (reciprocal of the $^1n\pi^*$ S_1 lifetime) for HPA and HPDP in neat as well as H_2O/MeCN mixed solvent and take this as an upper limit value. This value is very close to the result obtained using the triplet quenching method as reported by Givens, Wirz, and co-workers.[8,9,10b,11]

The stronger $^1n\pi^*$ and $^1\pi\pi^*$ vibronic coupling in H_2O/MeCN mixed solvent than in neat MeCN could also account for the increased intensity ratio of the $^1n\pi^*$ to $^1\pi\pi^*$ fluorescence in the former to latter solvent system. Our KTRF result shows that relative fluorescence integration of the $^1n\pi^*$ to $^1\pi\pi^*$ band increases (by ~3 times larger in H_2O/MeCN mixed solvent related to neat MeCN, Table 1) as the two bands shift close to each other. Assuming a similar oscillator strength for the $^1\pi\pi^*$ fluorescence transition, this implies an enhancement of the $^1n\pi^*$ oscillator strength associated with the smaller $^1n\pi^*$ to $^1\pi\pi^*$ energy gap. This is well within expectation considering that electronic transition between the S_0 and $^1n\pi^*$ states is symmetric forbidden for planar aromatic carbonyls but can derive some finite allowed nature via vibronic coupling with the nearby $^1\pi\pi^*$ state(s) (most probably the S_3 state here); the extent of the allowed character depends on the strength of the vibronic coupling that is substantially favored by the closer energy gap between the two states in H_2O/MeCN mixed than in neat MeCN solvent.[28−30,37,38,49,50] It is expected that this result here may spur further solution phase experimental and theoretical work on the singlet excited state properties for aromatic carbonyls especially in H-bonding solvents, since, to our knowledge, there has been little work reported on this aspect in the literature.

Since the triplet formation time is associated with the $^1n\pi^*$ lifetime decay (that is, ~2 and 1 ps for the two compounds in neat and H_2O/MeCN mixed solvents, respectively), there must be an additional process responsible for the much longer time scale (~7−12 ps) observed for the full development of the triplet TR^3 spectrum. By checking the early time spectra carefully and as shown in Figure 4, we found that temporal growth of the triplet band intensity is accompanied by a slight frequency upshift (by ~40 cm^{-1}) and bandwidth narrowing (by ~40 cm^{-1}) for HPA and HPDP in both H_2O/MeCN mixed and neat MeCN solvents (for details of these changes in spectral profile, the reader is referred to refs 60 and 61). Such an early time spectral change in Raman band profile is a characteristic indication to an excess energy relaxation process.[60,61,68−73] It has been shown that a typical time scale for this kind of relaxation is around 10 ps that matches well with the ~7−12 ps time constant obtained here. We therefore attributed the observed early stage $^3\pi\pi^*$ spectral evolution to combined dynamics involving growth of the triplet population and subsequent relaxation of excess energy (~11 000 cm^{-1}) introduced by 267 nm excitation and rapid ISC

(66) Shah, B. K.; Rodgers, M. A. J.; Neckers, D. C. *J. Phys. Chem. A* **2004**, *108*, ASAP.
(67) Wagner, P. J.; Kemppainen, A. E.; Schott, H. N. *J. Am. Chem. Soc.* **1973**, *95*, 5604−5614.
(68) Ma, C.; Kwok, W. M.; Matousek, P.; Parker, A. W.; Phillips, D.; Toner, W. T.; Towrie, M. *J. Raman Spectrosc.* **2001**, *32*, 115−123.
(69) Matousek, P.; Parker, A. W.; Towire, M.; Toner, W. T. *J. Chem. Phys*, **1997**, *107*, 9807−9817.
(70) Iwata, K.; Hamaguchi, H. *J. Phys. Chem. A* **1997**, *101*, 632−637.
(71) Hester, R. E.; Matousek, P.; Moore, J. N.; Parker, A. W.; Toner, W. T.; Towire, M. *Chem. Phys. Lett.* **1993**, *208*, 471−478.
(72) Weaver, W. L.; Huston, L. A.; Iwata, K.; Gustafson, T. L. *J. Phys. Chem.* **1992**, *96*, 8956−8961.
(73) Matousek, P.; Parker, A. W.; Towrie, M. *J. Chem. Phys.* **1997**, *107*, 9807−9817.

conversion. Given the closeness of the $^1n\pi^*$ and $^3\pi\pi^*$ energy levels, this implies, on the other hand, that the fluorescence observed in the KTRF spectra are from the vibronically hot $^1\pi\pi^*$ and $^1n\pi^*$ states consistent with the short singlet lifetimes preventing full relaxation of the emitting states. Due to the efficient ISC deactivation of the singlet state, relaxation of excess energy on the triplet manifold has been observed generally for various aromatic carbonyls in the solution phase, and our results here are consistent with these other observations.[74−77]

In summary, we suggest the following nonradiative pathway for the 267 nm photoexcitation of HPA and HPDP in solvent:

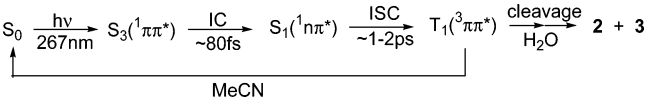

This scheme provides a consistent interpretation to the dynamics and related solvent dependence observed in the present KTRF and ps-TR[3] experiments. Our results show clearly that photophysical and photochemical processes of *p*HP phototriggers occur in well-separated time scales. The photophysical associated processes including photoexcitation, IC between the singlet excited states, ISC from the singlet to triplet, relaxation of excess energy, etc. take place in the femtosecond to early picosecond time regime and finish within tens of picoseconds. The deprotection related photochemistry is much slower and proceeds from the fully relaxed triplet on the several hundred picoseconds or nanosecond time scale depending on the kind of leaving group.

Except for the photochemistry step(s) occurring subsequently to the triplet generation in H_2O containing solvents, we found that the deactivation pathway shown in the scheme also applies to several closely related aromatic carbonyls. However, provided the complex dependence of fluorescence and ISC behavior on many factors, such as the solvent properties,[31−39] the temperature,[78] the electronic nature of the ring substituted groups, etc.,[28,29,67] further work is under way to understand the general nonradiative channels for a selected diverse range of aromatic carbonyls compounds.

D. Brief Discussion of Implications for the Deprotection Reaction. The observation that the decay rate of the $^3\pi\pi^*$ triplet is strongly leaving group dependent and is larger for HPDP than for HPA in H_2O/MeCN mixed solvent appears to lend support to the direct triplet heterolytic deprotection pathway proposed by Givens, Wirz, and co-workers.[11] This is because, as scaled by the pK_a value to describe the anion stability and leaving group ability, diethyl phosphate has been found to be a better leaving group than acetate.[79] However, our recent studies show that the triplet ps-TR[3] spectra of HPA and HPDP in neat MeCN closely resemble those of the "cage" HA and are barely leaving group dependent.[61] This has also been corroborated by theoretical calculations and has been interpreted to be due to the analogous electronic and structural properties of the triplet for the *p*HP phototriggers in terms of the *p*-hydroxyphenacyl chromophore.[60,61] Our calculations also revealed some structural and bonding changes associated with the leaving group on going from the ground to the triplet state. There is a slight lengthening of the C−O bond connecting the *p*HP cage and leaving groups and a significant variation in the relative orientation between the two parts. However, the extent of these changes were found to be not very sensitive to the kind of leaving group and rather similar for HPA and HPDP (for a detailed description of the triplet structure, the reader is referred to refs 60 and 61). This, on the other hand, implies that, upon the triplet formation, further processes are required to induce a favorable structural modification and charge redistribution to consequently trigger the cleavage and accompanying relevant rearrangement. The fact that *p*HP photorelease occurs only in H_2O containing solvent indicates that H_2O may act not only as solvent but also as a reactant and/or catalyst that could be the source of the driving force for the cleavage process.

Our KTRF results described in the preceding section indicate the important influence of intermolecular H-bonding on the radiative and nonradiative dynamics for the singlet excited states. It is thus reasonable to consider possible H-bonding effects on the triplet and subsequent deprotection reaction. Although the general character of the triplet TR[3] spectrum is comparable in neat MeCN and H_2O/MeCN mixed solvents, a careful examination of the spectra displayed in Figure 2 shows some small but clear differences (such as relative intensity distribution of Raman bands) in the two solvents that are likely associated with the H-bonding interaction.[11,12] But the observation that the triplet spectra in H_2O/MeCN mixed solvent are little different for HPA and HPDP indicates the H-bonding modification of the triplet in terms of the *p*HP chromophorm is similar for *p*HP phototriggers with different leaving groups and thus is unlikely to fully account for the leaving group dependent deprotection processes.

Plausible processes accounting for the water and leaving group dependent dynamics quenching the $^3\pi\pi^*$ triplet could be (i) water assisted and/or catalyzed direct heterolysis or homolysis followed by rapid electron transfer cleavage of the leaving group, (ii) deprotonation and/or protonation of the triplet state. Regarding the first possibility, we note that solvent-assisted heterolysis cleavage of the leaving group, including the phosphate and acetate studied here, was postulated previously to account for photocleavage of (7-methoxycoumarin-4-yl) methyl (MCM) caged compounds;[79] the photoheterolysis cleavage mechanism has also been suggested for several other system bearing the phosphate as a leaving group.[80−82] In addition, a very recent combined experimental and theoretical study by Phillips and co-workers demonstrates that water-catalyzed solvation of a leaving group into ions is the driving force responsible for photodecomposition of isopolyhalomethanes in water solvated environments.[83] With regards to the second possibility, it is essential to emphasize the well-established fact that phenols become stronger acids upon photoexcitation, while

(74) (a) Turek, A. M.; Krishnamoorthy, G.; Phipps, K.; Saltiel, J. *J. Phys. Chem. A* **2002**, *106*, 6044−6052. (b) Sun, Y.-P.; Sears, D. F., Jr.; Saltiel, J. *J. Am. Chem. Soc.* **1989**, *111*, 706−711.
(75) Wolf, M. W.; Legg, K. D.; Brown, R. E.; Singer, L. A.; Parks, J. H. *J. Am. Chem. Soc.* **1975**, *97*, 4490−4497.
(76) Kiritani, M.; Yoshii, T.; Hirota, N.; Baba, M. *J. Phys. Chem.* **1994**, *98*, 11265−11268.
(77) Sneh, O.; Cheshnovsky, O. *J. Phys. Chem.* **1991**, *95*, 7154−7164.
(78) Jones, P. F.; Calloway, A. R. *J. Am. Chem. Soc.* **1970**, *92*, 4997−4998.
(79) Schade, B.; Hagen, V.; Schmidt, R.; Herbrich, R.; Krause, E.; Eckardt, T.; Bendig, J. *J. Org. Chem.* **1999**, *64*, 9109−9117.
(80) Newcomb, M.; Horner, J. H.; Whitted, P. O.; Crich, D.; Huang, X.; Yao, Q.; Zipse, H. *J. Am. Chem. Soc.* **1999**, *121*, 10685−10694.
(81) Whitted, P. O.; Horner, J. H.; Newcomb, M.; Huang, X.; Crich, D. *Org. Lett.* **1999**, *1*, 153−156.
(82) Horner, J. H.; Taxil, E.; Newcomb, M. *J. Am. Chem. Soc.* **2002**, *124*, 5402−5410.

the $^3\pi\pi^*$ triplet of aromatic carbonyls become stronger bases.[11,12,84−86] It is therefore reasonable to deduce that, for *p*HP compounds with the two functional groups (hydroxy and carbonyl) on the same chromophore, protonation at the carbonyl oxygen and deprotonation at the hydroxy site is highly likely to occur after photoexcitation.[12,86] Such processes could formally manifest themselves as the so-called ESIPT suggested by Wan and co-workers[12] but on the triplet rather than the singlet manifold because of the rapid ISC dynamics as demonstrated in our present study. Indeed, the deprotonation related reaction has been reported for the HA cage by Wirz and co-workers[11] and proposed for HPA by Wan and co-workers.[12] However, we note that there remains some uncertainty about the explicit correlation between the deprotonation and cleavage reaction. It appears that the deprotonation process displays little leaving group dependence and thus could function as a competing process with the cleavage reaction to deactivate the triplet state. It is therefore reasonable to suggest that the overall photochemical pathway and deprotection efficiency for a specific *p*HP phototrigger could be mostly controlled by a dynamic competition between the heterolysis cleavage and deprotonation process. In this sense, the leaving group ability and therefore the cleavage rate and rate of the deprotection would be the major factors in determining the *p*HP photochemistry. Further TR^3 work on the picosecond to nanosecond time scale is in progress to more fully address the cleavage mechanism and relevant rearrangement reaction.

Conclusion

By using fs-KTRF spectroscopy to monitor the singlet excited states and ps-KTR^3 to detect the triplet state, the present investigation reports a combined ultrafast time-resolved study on photophysical processes of two *p*HP caged compounds HPDP and HPA in neat MeCN and H_2O/MeCN mixed solvent. These results show that 267 nm excitation leads to instantaneous population of the $^1\pi\pi^*$ S_3 state that has a lifetime of ∼80 fs and is deactivated by internal conversion to the $^1n\pi^*$ S_1 state. The $^1n\pi^*$ lifetime was found to be ∼1 and 2 ps in H_2O/MeCM mixed and neat MeCN, respectively. Spectral properties of the $^1\pi\pi^*$ and $^1n\pi^*$ fluorescence transitions are strongly influenced by the solvent H-bonding strength indicating the importance of intermolecular H-bonding interaction for the excited molecules. Dynamic correlation between the singlet decay and triplet formation indicates a direct $^1n\pi^* \rightarrow {}^3\pi\pi^*$ ISC mechanism with the ISC rate estimated to be $\sim 5 \times 10^{11}$ s^{-1} in both solvents. The shorter $^1n\pi^*$ lifetime in the H_2O/MeCN mixed solvent than in neat MeCN was interpreted as being due to the increased rate of internal conversion relative to ISC to deactivate the $^1n\pi^*$. This increased IC is likely caused by the substantially reduced $^1n\pi^*$ and $^1\pi\pi^*$ gap in the H_2O/MeCN mixed solvent than in neat MeCN solvent (the proximity effect). Spectral evolution of the $^3\pi\pi^*$ triplet Raman bands on the early tens picosecond time scale was attributed to the combined dynamics of the development of the triplet population and relaxation of the excess energy induced by the S_3 excitation and rapid ISC conversion. In H_2O/MeCN mixed solvent, the triplet lifetime was found to be ∼420 and 2130 ps for HPDP and HPA, respectively, substantially shorter than that in neat MeCN (150 and 137 ns for HPDP and HPA, respectively). This leaving group and solvent-dependent dynamic quenching of the $^3\pi\pi^*$ triplet is a clear indication for occurrence of the deprotection related photochemistry. The observations here provide direct experimental evidence that the photochemical step(s) takes place from the fully relaxed triplet and thus rules out the singlet mechanism for HPA and HPDP after 267 nm excitation. The results show clearly that the photophysics and photochemistry of *p*HP caged compounds proceed on a well-separated time scale. The photophysical steps occur on the femtosecond to tens picosecond time regime and are independent of the existence and kind of leaving group, whereas the deprotection related steps happen on the several hundreds picosecond to nanosecond and later time scales. The strong dependence of the deprotection on the leaving group ability suggests a heterolysis cleavage mechanism may be involved in the deprotection mechanism.

Acknowledgment. This research was done in the Ultrafast Laser Facility at the University of Hong Kong and supported by grants from the Research Grants Council of Hong Kong (HKU/7108/02P) and (HKU 1/01C) to D.L.P. and (HKU 7112/02P) and (HKU 7027/03P) to P.H.T.. W.M.K. thanks the University of Hong Kong for the award of a Postdoctoral Fellowship.

Supporting Information Available: Details for the synthesis and characterization of HPA and HDPD. Details for using log-normal function to simulate the experimentally measured KTRF spectra including (i) estimation of intensity ratio of the $^1n\pi^*$ to $^1\pi\pi^*$ fluorescence band and (ii) estimation of the overall fluorescence quantum yield. Additional spectral parameters obtained from the log-normal simulation of the fluorescence and absorption spectra are listed in Table S1. Fluorescence spectra of the $^1n\pi^*$ and $^1\pi\pi^*$ state calculated based on the KTRF spectra for HPA in neat MeCN with 267 nm excitation is displayed in Figure S1. Figure S2 shows a comparison of the normalized absorption spectra for HA, HPA, and HPDP in neat MeCN solvent. Figure S3 shows ps-KTR^3 spectra of HPA in neat MeCN and H_2O/MeCN (1:1 by volume) mixed solvent obtained with 267 nm excitation and 400 nm probe wavelength. Figure S4 shows comparison of early time ps-KTR^3 spectra of HPA in H_2O/MeCN (1:1 by volume) mixed solvent obtained with 267 nm excitation, 400 and 342 nm probe wavelength. This material is available free of charge via the Internet at http://pubs.acs.org.

JA0458524

(83) (a) Kwok, W. M.; Zhao, C.; Li, Y.-L.; Guan, X.; Phillips, D. L. *J. Chem. Phys.* **2004**, *120*, 3323−3332. (b) Kwok, W. M.; Zhao, C.; Li, Y.-L.; Guan, X.; Wang, D.; Phillips, D. L. *J. Am. Chem. Soc.* **2004**, *126*, 3119−3131. (c) Kwok, W. M.; Zhao, C.; Guan, X.; Li, Y.-L.; Du, Y.; Phillips, D. L. *J. Chem. Phys.* **2004**, *120*, 9017−9032.
(84) (a) Canonica, S.; Hellrung, B.; Wirz, J. *J. Phys. Chem. A* **2000**, *104*, 1226−1232. (b) Ramseier, M.; Senn, P.; Wirz, J. *J. Phys. Chem. A* **2003**, *107*, 3305−3315.
(85) Leigh, W. J.; Lathioor, E. C.; St. Pierre, M. J. *J. Am. Chem. Soc.* **1996**, *118*, 12339−12348.
(86) Das, P. K.; Encinas, M. V.; Scaiano, J. C. *J. Am. Chem. Soc.* **1981**, *103*, 4154−4162.